van der Waals interactions between excited-state atoms and dispersive dielectric surfaces

M. Fichet, F. Schuller, D. Bloch, and M. Ducloy
Laboratoire de Physique des Lasers, URA 282 du CNRS, Université Paris-Nord, 93430 Villetaneuse, France
(Received 19 April 1994; revised manuscript received 26 September 1994)

van der Waals interactions between atoms and dielectric surfaces are reinvestigated. To describe the nonretarded interaction potential between a dispersive dielectric surface and an atom in an arbitrary internal energy state, we derive a general expression in terms of an integral, over *real* frequency, of the combined atom and surface polarizabilities. It is shown that, for excited atoms, the expression is equivalent to the one obtained by Wylie and Sipe [Phys. Rev. A **32**, 2030 (1985)]. We thus demonstrate how to extend this approach to excited atoms interacting with *birefringent* dielectrics. For isotropic dielectrics, a method of integration in closed form allows us to derive an approximate formula for the van der Waals interaction constant in terms of resonance frequencies and oscillator strengths of both the atom and the dielectric. Frequency-dependent "*dielectric reflection*" coefficients are introduced for virtual atomic dipole couplings either in absorption or in emission. In absorption, the reflection coefficient is always positive and smaller than unity. In emission, it may take arbitrary values, positive or negative (corresponding to van der Waals repulsion). Such a behavior is shown to be related to resonant excitation exchange between the atomic system and the dielectric medium, when an atomic transition frequency gets in resonance with a dielectric absorption band. Numerical calculations performed for the cesium-sapphire system are shown to be in good agreement with data obtained by selective-reflection spectroscopy. Finally, experimental tests of the birefringent character of the sapphire response are discussed.

PACS number(s): 42.50.−p, 42.25.Gy

I. INTRODUCTION

Since the pioneering work of Lennard-Jones [1], the theory of van der Waals (vW) interactions between isolated atoms and solid-state surfaces has been developed by many authors over the past decades [2–13]. In the nonretarded regime, the interaction between an atom and a perfectly reflecting surface can be viewed as resulting from the coupling of the atomic dipole with its electrostatic image in the surface. Due to the image correlation, the dipole–induced-dipole interaction varies like z^{-3} (z is the atom-surface distance). Most of the previous theoretical works have dealt with the interaction of ground-state atoms with metallic or dielectric surfaces, for both nonretarded and retarded vW forces [1–6,11]. Resonance-level atoms interacting with perfect conductors or metals have also been investigated, in relation with quantum electrodynamic studies in the presence of an interface (cavity QED) [7–10,12–14]. Of particular interest is the quite complete study performed by Wylie and Sipe [12], who derived a general expression of atomic level shifts in terms of correlation functions from linear-response theory.

Many experimental studies of the vW interactions between ground-state atoms and solid-state surfaces have been performed [15]. On the other hand, recent experimental investigations on selective-reflection spectroscopy at an interface between a dielectric surface and a dilute alkali-metal vapor [16–18] have attracted a renewed interest in the problem of excited-state atoms interacting with dielectric media. The experimental results are well interpreted by assuming a nonretarded vW potential varying in z^{-3}. However, the precise interpretation of the atomic frequency shift requires that one take into account the full, complex dielectric response at all the wavelengths, due to the fact that some excited atomic transitions may lie inside the absorption bands of the dielectric medium.

In this article, we consider the nonretarded interaction potential between an atom in an energy level $|a\rangle$ and a dielectric surface characterized by a frequency-dependent, complex, dielectric constant $\varepsilon(\omega)$. We derive a general expression valid for an arbitrary atomic level (Sec. II). The case of birefringent dielectrics is also considered. Model calculations are performed in Sec. III to get an approximate analytical expression of the vW interaction constant C_3 in terms of resonance frequencies and oscillator strengths of both the atom and the dielectric. Sections IV and V are thus devoted to the particular case of the dielectric response of the sapphire and to the calculation of sapphire-induced energy shifts of cesium excited states, including a comparison with the experimental results. In Appendix A, the limit case of a dilute dielectric medium is shown to give the well-known vW potential between two atoms.

II. POTENTIAL ENERGY OF ATOMS NEAR A DIELECTRIC SURFACE

A. The electrostatic image model

Let us recall that, in electrostatics, the effect of an arbitrary flat dielectric surface (dielectric constant $\varepsilon_s > 1$) on a charge q located in vacuum at distance z from the sur-

 ©1995 The American Physical Society

face can be modeled by assuming the presence of an image charge $-q[(\varepsilon_s-1)/(\varepsilon_s+1)]$, located symmetrically at position $-z$ [19]. Similarly, the effect of the dielectric surface on an electric dipole $\boldsymbol{\mu}$ is equivalent to an image dipole $\boldsymbol{\mu}^I$ with components parallel to the surface

$$\mu^I_{x,y}=-\frac{\varepsilon_s-1}{\varepsilon_s+1}\mu_{x,y} \tag{1}$$

and normal to the surface

$$\mu^I_z=\frac{\varepsilon_s-1}{\varepsilon_s+1}\mu_z \ . \tag{2}$$

This leads to a dipole-image dipole interaction energy of the form

$$V_{\rm cl}=-\frac{\varepsilon_s-1}{\varepsilon_s+1}\frac{\mu_x^2+\mu_y^2+2\mu_z^2}{16z^3} \ . \tag{3}$$

The case of a perfect reflector is given by the limit $\varepsilon_s\to\infty$.

The corresponding quantum-mechanical interaction operator V is given by Eq. (3), where $\boldsymbol{\mu}$ is now the atom electric dipole moment operator. At first perturbation order, the energy shift of the atomic level $|a\rangle$ is given by

$$\begin{aligned}\langle a|V|a\rangle&=-\frac{\varepsilon_s-1}{\varepsilon_s+1}\frac{\langle a|\boldsymbol{\mu}^2+\mu_z^2|a\rangle}{16z^3}\\&=-\frac{1}{16z^3}\frac{\varepsilon_s-1}{\varepsilon_s+1}\sum_n[|\mu_x^{an}|^2+|\mu_y^{an}|^2+2|\mu_z^{an}|^2]\end{aligned} \tag{4}$$

in which

$$\mu^{an}_{x_i}=\langle a|\mu_{x_i}|n\rangle \tag{5}$$

is the $|a\rangle\to|n\rangle$ transition dipole moment along direction x_i and the summation is performed over all atomic levels $|n\rangle$ connected by electric dipole transitions to $|a\rangle$. Equation (4) is valid if we assume the dielectric to respond instantaneously at any atomic transition frequency. When some of the electric dipole transitions of the atom lie inside the absorptive or dispersive ranges of the medium, the dielectric response is characterized by a frequency-dependent, complex, dielectric permittivity $\varepsilon(\omega)$ and Eq. (4) no longer applies.

B. van der Waals interactions between ground-state atoms and dispersive dielectric media

The vW interactions between an atom in the ground state and a dielectric surface has been derived by several authors [4–6,11,12] on the basis of either QED approaches or the linear-response theory using quantum-mechanical perturbation approach. In the nonretarded regime, the vW interaction may be simply expressed as an integral, over pure imaginary frequencies (iu), of the optical responses of the atom and the solid:

$$\begin{aligned}V_g(z)=-\frac{\hbar}{16\pi z^3}\int_0^\infty du[&\alpha^g_{xx}(iu)+\alpha^g_{yy}(iu)\\&+2\alpha^g_{zz}(iu)]\frac{\varepsilon(iu)-1}{\varepsilon(iu)+1} \ .\end{aligned} \tag{6}$$

$\alpha^g_{x_ix_i}$ represents the component along x_i of the tensorial polarizability of the ground-state atom. For an isotropic ground state, $\alpha^g_{xx}=\alpha^g_{yy}=\alpha^g_{zz}=\alpha^g$ and Eq. (6) reduces to [4–6]

$$V_g(z)=-\frac{\hbar}{4\pi z^3}\int_0^\infty\alpha^g(iu)\frac{\varepsilon(iu)-1}{\varepsilon(iu)+1}du \ . \tag{7}$$

One may introduce in Eq. (6) the well-known expression for the polarizability of the ath atomic state

$$\alpha^a_{xx}(\omega)=\frac{2}{\hbar}\sum_n|\mu_x^{an}|^2\frac{\omega_{an}}{\omega_{an}^2-\omega^2} \tag{8}$$

in which $\omega_{an}=(E_n-E_a)/\hbar$ is the $a\to n$ transition frequency (positive for $E_n>E_a$, negative for $E_n<E_a$) and μ_x^{an} is defined by Eq. (5). We obtain

$$\begin{aligned}V_g(z)=-\frac{1}{8\pi z^3}\sum_n(&|\mu_x^{gn}|^2+|\mu_y^{gn}|^2+2|\mu_z^{gn}|^2)\\&\times\int_0^\infty\frac{\varepsilon(iu)-1}{\varepsilon(iu)+1}\frac{\omega_{gn}}{\omega_{gn}^2+u^2}du \ ,\end{aligned} \tag{9}$$

which can be also written as

$$V_g(z)=-\frac{1}{16z^3}\sum_n(|\mu_x^{gn}|^2+|\mu_y^{gn}|^2+2|\mu_z^{gn}|^2)r(\omega_{gn}) \tag{10}$$

if we introduce a *frequency-dependent "dielectric reflection" coefficient* as

$$r(\omega_0)=\frac{2}{\pi}\int_0^\infty\frac{\varepsilon(iu)-1}{\varepsilon(iu)+1}\frac{\omega_0}{\omega_0^2+u^2}du \tag{11}$$

(in which $\omega_0=\omega_{gn}>0$). For long wavelengths (electrostatic limit $\omega_0\to0$), $r_0=[\varepsilon(0)-1]/[\varepsilon(0)+1]$, where $\varepsilon(0)$ is the *static* dielectric constant. It follows, from the properties of $\varepsilon(\omega)$ [20], that $\varepsilon(iu)$ is real, positive, and falls off monotonically to one as u increases. Thus $r(\omega_0)$ is also monotonically decreasing from $r_0(\omega_0=0)$ to zero $(\omega_0\to\infty)$. For $\varepsilon(\omega)=\varepsilon_s$, $r(\omega)=(\varepsilon_s-1)/(\varepsilon_s+1)$, and Eq. (10) reduces to Eq. (4).

The integral of Eq. (11) over the imaginary frequency axis can be turned into an integral over *real* frequency axis by using the integration contour of Fig. 1. For this, one notes that the function $[\varepsilon(\omega)-1]/[\varepsilon(\omega)+1]$ has no pole in the upper complex plane. It can be shown indeed [20] that, because of causality principle, $\varepsilon(\omega)$ is not real in the upper complex plane, except on the imaginary axis, where ε is real and positive. Thus, by integrating $\{[\varepsilon(\omega)-1]/[\varepsilon(\omega)+1]\}[\omega_0/(\omega_0^2-\omega^2)]$ over the contour of Fig. 1, one obtains r as

$$r(\omega_0)=\frac{2}{\pi}\mathrm{P}\int_0^\infty\mathrm{Im}\frac{\varepsilon(\omega)-1}{\varepsilon(\omega)+1}\frac{\omega_0}{\omega_0^2-\omega^2}d\omega+\mathrm{Re}\frac{\varepsilon(\omega_0)-1}{\varepsilon(\omega_0)+1} \ . \tag{12}$$

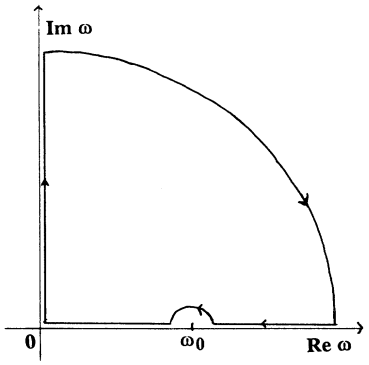

FIG. 1. Integration contour for turning the integral of Eq. (11) into an integral over the real frequency axis.

In Eq. (12), P stands for the principal value of the integral and Re and Im denote real and imaginary parts, respectively.

C. Excited-state atom interaction

Equations (10) and (12), yielding the nonretarded vW interaction for a ground-state atom, are generalizable to *any* atomic state since they are expressed in terms of *real* atomic and dielectric frequencies. They can be obtained directly via Fourier-transform methods from quantum-mechanical perturbation theory applied to any energy level of the atom-dielectric system. The vW shift for an excited level $|e\rangle$ is

$$V_e(z)=-\frac{1}{16z^3}\sum_{n'}(|\mu_x^{en'}|^2+|\mu_y^{en'}|^2+2|\mu_z^{en'}|^2)r(\omega_{en'}) , \tag{13}$$

with r given by Eq. (12). Let us note that, now in the summation on the right-hand side of Eq. (13), there may be a state $|n'\rangle$ of lower energy than that of state $|e\rangle$, which means $\omega_{en'}<0$ (i.e., virtual dipole coupling in *emission*). For $\omega_{en'}<0$, $r(\omega_{en'})$, as given by Eq. (12), is no longer equivalent to expression (11). Indeed, when carrying out the reverse transformation by means of the integration contour of Fig. 1, one easily shows that, for *negative* frequency, the dielectric reflection coefficient is given by

$$r(-|\omega_0|)=-\frac{2}{\pi}\int_0^\infty \frac{\varepsilon(iu)-1}{\varepsilon(iu)+1}\frac{|\omega_0|}{\omega_0^2+u^2}du +2\,\mathrm{Re}\frac{\varepsilon(|\omega_0|)-1}{\varepsilon(|\omega_0|)+1} , \tag{14}$$

where we have used the well-known relation $\varepsilon^*(\omega^*)=\varepsilon(-\omega)$. It is shown in Appendix A that, in the limit case of a noninteracting, dilute dielectric medium, this expression allows us to derive the well-known binary vW potential between two different atoms [cf. Eq. (A3) and the following].

Relation (14), when inserted in Eq. (13), with the help of Eq. (8), yields the following potential energy:

$$V_e(z)=-\frac{\hbar}{16\pi z^3}\int_0^\infty du\,[\alpha_{xx}^e(iu)+\alpha_{yy}^e(iu)+2\alpha_{zz}^e(iu)]\frac{\varepsilon(iu)-1}{\varepsilon(iu)+1} -\frac{1}{8z^3}\sum_{n'}[|\mu_x^{en'}|^2+|\mu_y^{en'}|^2+2|\mu_z^{en'}|^2] \times\mathrm{Re}\left[\frac{\varepsilon(\omega_{en'})-1}{\varepsilon(\omega_{en'})+1}\right]\Theta(-\omega_{en'}) , \tag{15}$$

where Θ is the Heaviside function. This expression was first derived by Wylie and Sipe [12], who gave a very general approach (in the retarded and nonretarded regime) of the interaction between atoms and solid-state surfaces. They have interpreted this energy shift by associating the first part of the right-hand side of Eq. (15) with the forces induced by pure *quantum-mechanical fluctuations* (which yield the *only* shift for ground state or metastable atoms), while they have shown that the second part, coming from atomic transitions associated with *emission* processes, is the quantum-mechanical analog of the energy shift of a *classical* oscillating dipole, interacting with a solid-state surface. Our approach shows that both Eq. (9) for the ground-state atom and Eq. (15) for excited state derive from a unique potential, which can be expressed in terms of real frequency [Eq. (12)]. The general meaning of Eqs. (10)–(15) will be analyzed in more detail when we will consider their application to a particular dielectric.

D. Birefringent dielectrics

The interaction between a ground-state atom and an anisotropic solid has been derived by several authors [21,22]. They have shown that, for a homogeneous birefringent dielectric with the symmetry axis normal to the interface, Eqs. (6) and (7) still apply if one replaces ε by $\bar{\varepsilon}$, with

$$\bar{\varepsilon}(iu)=[\varepsilon_\parallel(iu)\varepsilon_\perp(iu)]^{1/2} , \tag{16}$$

where $\varepsilon_\parallel$ and $\varepsilon_\perp$ are the dielectric permittivities for electric fields parallel and normal to the interface, respectively. This leads to a "dielectric image" coefficient for the ground state similar to Eq. (11)

$$\bar{r}(\omega_0)=\frac{2}{\pi}\int_0^\infty \frac{\bar{\varepsilon}(iu)-1}{\bar{\varepsilon}(iu)+1}\frac{\omega_0}{\omega_0^2+u^2}du . \tag{17}$$

Note that, since $\varepsilon(iu)$ is real and positive, $\bar{\varepsilon}(iu)$ is univocally defined by Eq. (16).

A generalization to the excited state is easily performed via the procedure detailed in Sec. II B to transform Eq. (17) into an integral over real frequencies

$$\bar{r}(\omega_0)=\frac{2}{\pi}\mathrm{P}\int_0^\infty \mathrm{Im}\frac{\bar{\varepsilon}(\omega)-1}{\bar{\varepsilon}(\omega)+1}\frac{\omega_0}{\omega_0^2-\omega^2}d\omega+\mathrm{Re}\frac{\bar{\varepsilon}(\omega_0)-1}{\bar{\varepsilon}(\omega_0)+1} . \tag{18}$$

In Eq. (18), $\bar{\varepsilon}(\omega)$, now complex, is given by the determination of $[\varepsilon_\parallel(\omega)\varepsilon_\perp(\omega)]^{1/2}$, which analytically extends $\bar{\varepsilon}(iu)$ over the upper complex plane of Fig. 1. Equation

(18) leads to a reflection coefficient for negative frequencies (corresponding to dipole coupling in *emission*) similar to Eq. (14), with ε replaced by $\bar{\varepsilon}$.

In the electrostatic limit ($\omega_0 \to 0$), $\bar{r}$ is equal to $(\bar{\varepsilon}_s - 1)/(\bar{\varepsilon}_s + 1)$ with $\bar{\varepsilon}_s = \sqrt{\varepsilon_{\parallel s}\varepsilon_{\perp s}}$. This result can be obtained by extending the image model to birefringent dielectrics, which is possible if the birefringence axis is normal to the surface (Fig. 2). Indeed the cylindrical symmetry around the surface normal and the continuity conditions on the interface for both the tangential electric field and the normal displacement field allow one to show that for a charge q at distance z from the interface (i) the field inside the birefringent dielectric [23] is equivalent to that produced by a fictitious charge $q_D = [2\bar{\varepsilon}_s/(\bar{\varepsilon}_s + 1)]q$ located at distance $z_D = z(\varepsilon_{\perp s}/\varepsilon_{\parallel s})^{1/2}$ from the surface and (ii) the field in the vacuum is equivalent to the one produced by the charge q and an image charge $q_I = -q(\bar{\varepsilon}_s - 1)/(\bar{\varepsilon}_s + 1)$ located at position $-z$. This shows that for an electric dipole μ, the interaction potential with birefringent dielectrics is given by Eq. (3), with ε_s replaced $\bar{\varepsilon}_s$.

III. MODEL CALCULATIONS

In this section we consider an isotropic dielectric in which ε, as a function of ω, can be modeled by the usual expression

$$\varepsilon(\omega) = 1 + C + \sum_n \frac{f_n \omega_n^2}{\omega_n^2 - \omega^2 - i\gamma_n \omega} , \tag{19}$$

where C is a constant and the third term on the right-hand side describes resonances in the dielectric medium around frequencies ω_n, with f_n and γ_n the strengths and widths of these resonances, respectively. Let us first consider a model with a single resonance. Then we obtain, after some elementary algebra,

$$f(\omega) = \mathrm{Im}\frac{\varepsilon(\omega) - 1}{\varepsilon(\omega) + 1} = \frac{2 f_1 \gamma_1 \omega_1^2}{(2+C)^2} \frac{\omega}{\left[\left(1 + \frac{f_1}{2+C}\right)\omega_1^2 - \omega^2\right]^2 + \gamma_1^2 \omega^2} . \tag{20}$$

By introducing the quantities

$$K_1 = \frac{2 f_1 \gamma_1 \omega_1^2}{(2+C)^2} , \quad \Omega_1^2 = \left(1 + \frac{f_1}{2+C}\right)\omega_1^2 , \tag{21}$$

we thus have

$$f(\omega) = K_1 \frac{\omega}{(\Omega_1^2 - \omega^2)^2 + \gamma_1^2 \omega^2} . \tag{22}$$

We first evaluate the integral in Eq. (12) by using the identity

$$\mathrm{P}\int_0^\infty f(\omega)\frac{1}{\omega_0^2 - \omega^2} d\omega = \int_0^\infty [f(\omega) - f(|\omega_0|)]\frac{1}{\omega_0^2 - \omega^2} d\omega . \tag{23}$$

With $f(\omega)$ defined by Eq. (22) we find

$$[f(\omega) - f(|\omega_0|)]\frac{1}{\omega_0^2 - \omega^2} = \frac{K_1}{D(\omega) D(\omega_0)(|\omega_0| + \omega)} \times [-\Omega_1^4 + \omega|\omega_0|(-2\Omega_1^2 + \omega^2 + \omega|\omega_0| + \omega_0^2 + \gamma_1^2)] , \tag{24}$$

where we have set $D(\omega) = (\Omega_1^2 - \omega^2)^2 + \gamma_1^2 \omega^2$.

We now consider the limiting case where the resonance around Ω_1 is extremely narrow, i.e., its width is negligible compared to all other characteristic frequencies of the system. In particular, the atomic frequency $|\omega_0|$ is assumed to lie outside the resonance in the dielectric. Then we may neglect γ_1^2 in the last factor on the right-hand side of Eq. (24) and, since the relevant values of ω are close to Ω_1, use the approximation $\Omega_1^4 \approx \omega\Omega_1^3$ and $-2\Omega_1^2 + \omega^2 + \omega|\omega_0| \approx -\Omega_1^2 + \Omega_1|\omega_0|$. Hence we write

$$[f(\omega) - f(|\omega_0|)]\frac{1}{\omega_0^2 - \omega^2} = K_1 \frac{\omega_0^2 - \Omega_1^2}{D(\omega_0)} \frac{\omega}{D(\omega)} .$$

If we further neglect the term $\gamma_1^2 \omega_0^2$ in the expression for $D(\omega_0)$ so that we have

$$\frac{\omega_0^2 - \Omega_1^2}{D(\omega_0)} = \frac{1}{\omega_0^2 - \Omega_1^2} ,$$

the integral defined by Eq. (23) takes the form

$$\mathrm{P}\int_0^\infty f(\omega)\frac{1}{\omega_0^2 - \omega^2} d\omega = \frac{K_1}{\omega_0^2 - \Omega_1^2}\int_0^\infty \frac{\omega}{D(\omega)} d\omega . \tag{25}$$

In the limit of vanishing γ_1, the calculation of the remaining integral yields the value $\pi/2\gamma_1\Omega_1$. Hence we obtain the expression

$$\mathrm{P}\int_0^\infty f(\omega)\frac{1}{\omega_0^2 - \omega^2} d\omega = \frac{K_1}{\omega_0^2 - \Omega_1^2}\frac{\pi}{2\gamma_1\Omega_1} . \tag{26}$$

It remains to evaluate the second term on the right-hand side of Eq. (12) for which we use again the approximation of negligible width of the resonance. We then have

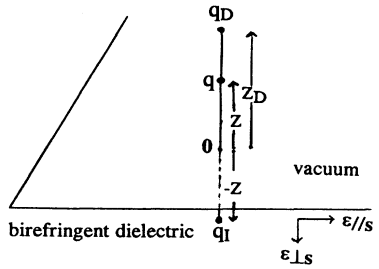

FIG. 2. Equivalent charges in the case of a birefringent dielectric.

$$\mathrm{Re}\frac{\varepsilon(\omega_0)-1}{\varepsilon(\omega_0)+1}=-\frac{(f_1+C)\omega_1^2-\omega_0^2 C}{(2+C)(\omega_0^2-\Omega_1^2)} . \tag{27}$$

By adding the expressions for the two terms we thus obtain the final result

$$r(\omega_0)=\frac{2}{2+C}\frac{1}{\omega_0^2-\Omega_1^2} \times\left[\frac{\omega_0 f_1\omega_1^2}{(2+C)\Omega_1}-\frac{(f_1+C)\omega_1^2-\omega_0^2 C}{2}\right], \tag{28}$$

where in Eq. (26) K_1 has been replaced by its value as given by Eq. (21). This result with $\omega_0=\omega_{en'}$ can now be substituted into Eq. (13) for the van der Waals potential.

In the more realistic case where $\varepsilon(\omega)$ possesses several resonances at values ω_n, there is no simple expression relating $f(\omega)$ to the quantities C and ω_n. However, if the resonances are sufficiently narrow, we can approximate $f(\omega)$ as a sum of Lorentzian-type resonances by writing it in the form

$$f(\omega)=\sum_n K_n\frac{\omega}{(\Omega_n^2-\omega^2)^2+\Gamma_n^2\omega^2} , \tag{29}$$

in analogy to the single resonance case. Note, however, that in contrast to this latter case, the damping constants are different from those of the expression for $\varepsilon(\omega)$. For the integral the result of Eq. (26) can then again be used so that we have

$$\mathrm{P}\int_0^\infty\frac{f(\omega)}{\omega_0^2-\omega^2}d\omega=\frac{\pi}{2}\sum_n\frac{K_n}{(\omega_0^2-\Omega_n^2)\Gamma_n\Omega_n} \tag{30}$$

and

$$\mathrm{Re}\frac{\varepsilon(\omega_0)-1}{\varepsilon(\omega_0)+1}=\frac{C+\sum_n\frac{f_n\omega_n^2}{\omega_n^2-\omega_0^2}}{C+2+\sum_n\frac{f_n\omega_n^2}{\omega_n^2-\omega_0^2}} . \tag{31}$$

Expressions for K_n and Γ_n in the case of multiple resonances are derived in Appendix B. Then Eqs. (30), (31), and (12) give

$$r(\omega_0)=\omega_0\sum_n\frac{K_n}{(\omega_0^2-\Omega_n^2)\Gamma_n\Omega_n}+\frac{C+\sum_n\frac{f_n\omega_n^2}{\omega_n^2-\omega_0^2}}{C+2+\sum_n\frac{f_n\omega_n^2}{\omega_n^2-\omega_0^2}} . \tag{32}$$

Note that, for $\omega_0\to+\infty$, $r\to C/(C+2)$. This asymptotic value comes from the empirical choice made in the modeling of the dielectric constant [in Eq. (19), $\varepsilon\to 1+C$ for $\omega\to+\infty$].

IV. AN EXAMPLE OF DIELECTRIC RESPONSE: THE SAPPHIRE SURFACE

In this section, we apply the previous theoretical approach to predict the dielectric response of a sapphire surface. Sapphire is a birefringent material. The dielectric permittivities of the ordinary mode $\varepsilon_\parallel(\omega)$ and the extraordinary mode $\varepsilon_\perp(\omega)$ can be expressed via analytical equations of the type of Eq. (19), by using data given in the literature for the visible and infrared ranges ($\lambda>0.4$ μm) [24].

TABLE I. Resonances of sapphire dielectric constant (ω_i and γ_i are given in units of 10^{12} Hz) (from Ref. [24]).

	i	ω_i	γ_i	f_i
$\varepsilon_\parallel(\omega)$	1	11.55	0.17	0.3
	2	13.26	0.13	2.7
$C_\parallel=2.2$	3	17.07	0.34	3.0
	4	19.05	0.38	0.3
$\varepsilon_\perp(\omega)$	1	12.	0.24	6.8
$C_\perp=2.1$	2	17.54	0.61	1.7

$\varepsilon_\parallel(\omega)$ has four resonances and $\varepsilon_\perp(\omega)$ two resonances, the characteristic parameters (f_i,ω_i,γ_i) of which are

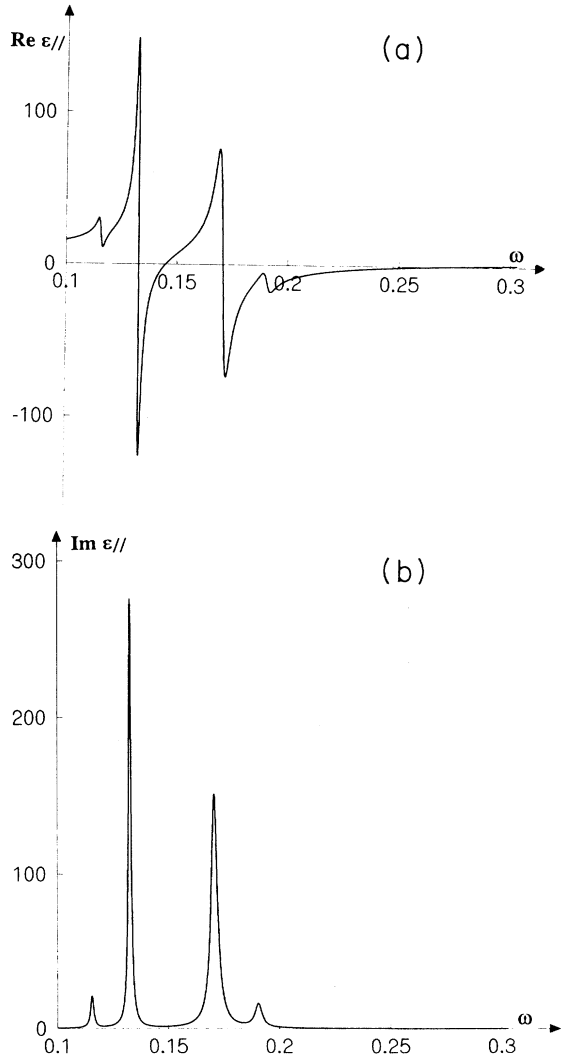

FIG. 3. $\varepsilon_\parallel(\omega)$ versus ω (in units of 10^{14} Hz) for the sapphire (a) real part and (b) imaginary part.

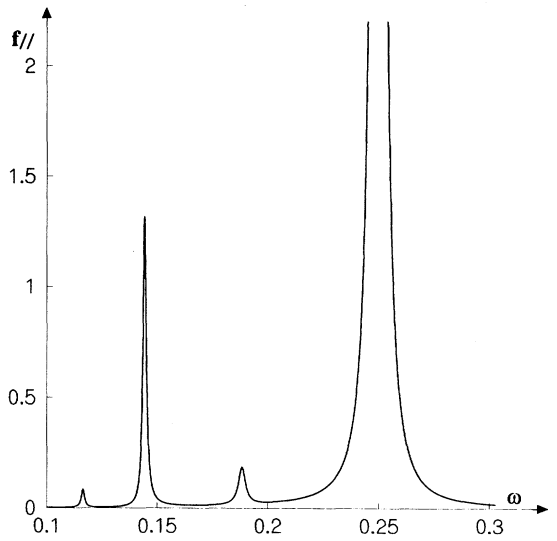

FIG. 4. $\mathrm{Im}[\varepsilon_{\parallel}(\omega)-1]/[\varepsilon_{\parallel}(\omega)+1]$ versus ω (in units of 10^{14} Hz) for sapphire.

given in Table I. As an example the frequency dependence of $\varepsilon_{\parallel}$ is given in Fig. 3.

The dielectric response of a plane sapphire interface is characterized by the function $F(\omega)=[\varepsilon(\omega)-1]/[\varepsilon(\omega)+1]$. Its imaginary part $f(\omega)=\mathrm{Im}F(\omega)$ is given in Fig. 4 for an ordinary index $f_{\parallel}(\omega)$. The approximate expression of $f_{\parallel}(\omega)$ as a sum of Lorentzian-type resonances [Eq. (29)] yields values that cannot be distinguished in Fig. 4 from the exact representation of $f_{\parallel}(\omega)$ such as that calculated with $\varepsilon_{\parallel}(\omega)$ [Eq. (19)]. Note that in general $f(\omega)$ has resonances at frequencies Ω_n, which are *quite different* from the resonances of the *bulk* dielectric permittivity ω_n. *Surface* resonances are given by the roots of $\varepsilon(\omega)+1=0$ (with $\gamma_n=0$). The characteristic parameters of the resonances of $f_{\parallel}(\omega)$ and $f_{\perp}(\omega)$ are given in Table II.

In fact, we have shown in Sec. II that, for a birefringent dielectric, the important observable is $\bar{\varepsilon}(\omega)=\sqrt{\varepsilon_{\parallel}(\omega)\varepsilon_{\perp}(\omega)}$, which we present in Fig. 5. Note that, for all ω, we have chosen the root with a positive imaginary part. The general shape of these figures results from the mixing of the six resonances. For example, in Fig. 5(b) we can notice that $\omega_2^{\perp}$ and $\omega_3^{\parallel}$ are so close that they give only one resonance and that the wings of the resonances $\omega_2^{\parallel}$ and $\omega_3^{\parallel}$ contribute to the small peak between them.

TABLE II. Resonances of *plane sapphire interface* [Ω_j and Γ_j are given in units of 10^{12} Hz and K_j in units of $(10^{12}\ \mathrm{Hz})^3$].

	j	Ω_j	Γ_j	K_j
	1	11.63	0.17	2.73×10^{-2}
$f_{\parallel}(\omega)$	2	14.42	0.18	0.5885
	3	18.82	0.37	0.4423
	4	24.96	0.3	49.85
$f_{\perp}(\omega)$	1	15.25	0.4	3.668
	2	24.20	0.45	77.079

In Fig. 6, we draw the function $\bar{f}(\omega)=\mathrm{Im}[\bar{\varepsilon}(\omega)-1]/[\bar{\varepsilon}(\omega)+1]$, which presents seven maxima, the position of which coincides with the minima of $|\bar{\varepsilon}(\omega)+1|$. Note that, for birefringent dielectrics, we cannot get an approximate expression of the type of Eq. (29) for the function presented in Fig. 6.

In Figs. 7 and 8, we present the dielectric reflection coefficient defined in Sec. II by Eqs. (11) and (14) for $\omega>0$ and $\omega<0$ with

$$\varepsilon(iu)=1+C+\sum_n \frac{f_n\omega_n^2}{\omega_n^2+u^2+\gamma_n u}\ , \tag{33}$$

where we have introduced the parameters given at the be-

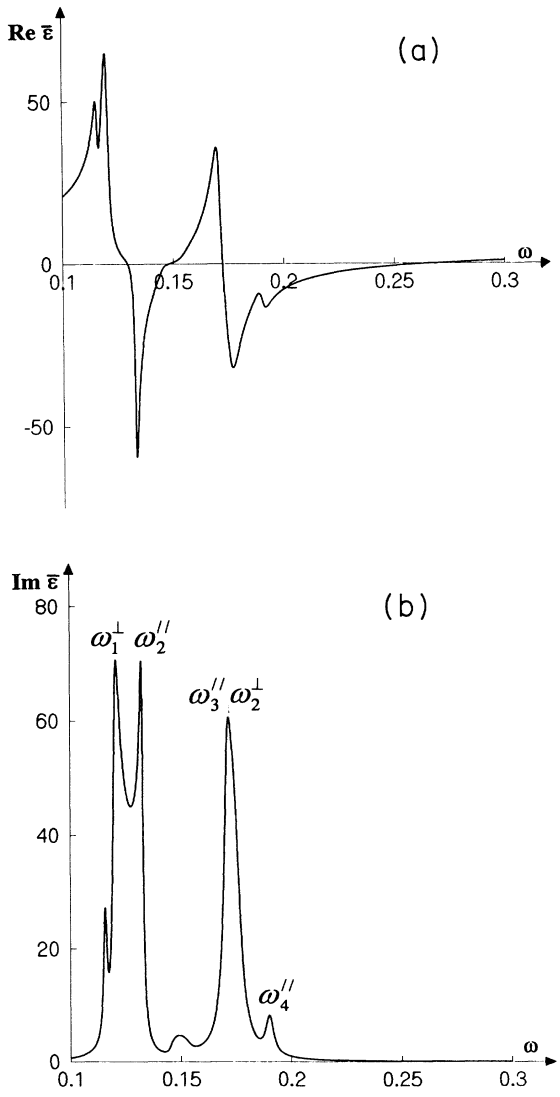

FIG. 5. $\sqrt{\varepsilon_{\parallel}(\omega)\varepsilon_{\perp}(\omega)}$ versus ω (in units of 10^{14} Hz) for the sapphire (a) real part and (b) imaginary part [$\omega_i^{\parallel}$ and $\omega_i^{\perp}$ indicate, respectively, the $\varepsilon_{\parallel}(\omega)$ and $\varepsilon_{\perp}(\omega)$ resonances positions].

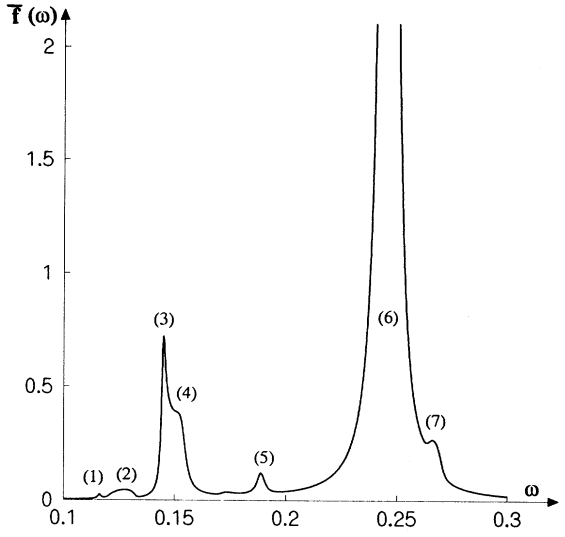

FIG. 6. $\mathrm{Im}\{[\sqrt{\varepsilon_{\parallel}(\omega)\varepsilon_{\perp}(\omega)}-1]/[\sqrt{\varepsilon_{\parallel}(\omega)\varepsilon_{\perp}(\omega)}+1]\}$ for sapphire (ω in units of 10^{14} Hz).

ginning of this section, respectively, for the ordinary mode $[r_{\parallel}(\omega)]$ and for the extraordinary mode $[r_{\perp}(\omega)]$. We note that $r(\omega>0)$ is, as predicted, a monotonically decreasing function starting from the static value $r_0(\omega=0)=[\varepsilon(0)-1]/[\varepsilon(0)+1]$; $[r_{\parallel}(0)=0.809$ and $r_{\perp}(0)=0.841]$. Note that, in *absorption* ($\omega>0$), the influence of sapphire birefringence is quite small and $r_{\parallel}$ and $r_{\perp}$ have *very close values.* This is not the case in *emission* ($\omega<0$), where r presents sharp variations around the associated surface resonances $\Omega_n^{\parallel}$ or $\Omega_n^{\perp}$: $r_{\parallel}(-|\omega|)$ varies from 22.36 to -21.47 for $|\omega|\approx\Omega_4^{\parallel}$ and $r_{\perp}(-|\omega|)$ varies from 15.76 to -15.05 for $|\omega|\approx\Omega_2^{\perp}$. This predicts a giant attraction or repulsion for an excited atom in front of the sapphire surface if this atom has a resonant transition for this ω value [25].

In Fig. 9, we compare $r_{\parallel}(\omega)$, given by Eq. (32) for our approximate method developed in Sec. III and Appendix B, to the exact results presented in Fig. 7. We can see that for the two cases ($\omega>0$ or $\omega<0$), the approximate method is excellent and can be used for the vW potential *except if the atom transitions coincide with the dielectric resonances.* The same conclusion can be reached for $r_{\perp}$.

The difference between $r_{\parallel}$ and $r_{\perp}$ shows the need to fully account for the birefringent behavior. In Fig. 10, we present the dielectric reflection coefficient for the birefringent case, where we have used Eqs. (11) and (14) with $\varepsilon(iu)=\bar{\varepsilon}(iu)$ given by Eq. (16). $\bar{r}(\omega>0)$ decreases monotonically from $\bar{r}(0)=0.826$ and is not very different from $r_{\parallel}$ and $r_{\perp}$. On the other hand, $\bar{r}(\omega<0)$ presents strong variations particularly around the peaks of $\bar{f}(\omega)$ (Fig. 6). We have noted the corresponding positions in Figs. 10 and 6 with the same number. On peak (3) at $|\omega|\approx 0.144\times10^{14}$ Hz ($\lambda=20.83$ μm), $\bar{r}(\omega)$ reaches 2.318. On peak (6), $\bar{r}(\omega)$ varies from 18 to -17 ($\bar{r}=0$ for $|\omega|=0.2456\times10^{14}$ Hz, $\lambda=12.21$ μm). From Table II we can infer that peak (3) mainly originates in resonance $\Omega_2^{\parallel}$ of the ordinary mode, while peak (6) comes from both $\Omega_4^{\parallel}$ and $\Omega_2^{\perp}$.

V. SAPPHIRE-INDUCED ENERGY SHIFT OF EXCITED CESIUM

It is worth applying the previous results to the cesium $6S_{1/2}-7P_{3/2}$ transition ($\lambda=455$ nm), for which detailed experimental results have been published [18], including evidence of the effects related to the nature of the dielectric medium. A striking feature is that an important contribution to the vW interaction ($7P_{3/2}\rightarrow6D_{5/2}$ coupling) lies in the sapphire absorption range. A detailed list of the various virtual couplings which contribute to the vW interaction for an ideal reflecting surface was previously given in [18]. It is schematically represented in Fig. 11.

Considering the case of a sapphire surface, one finds a

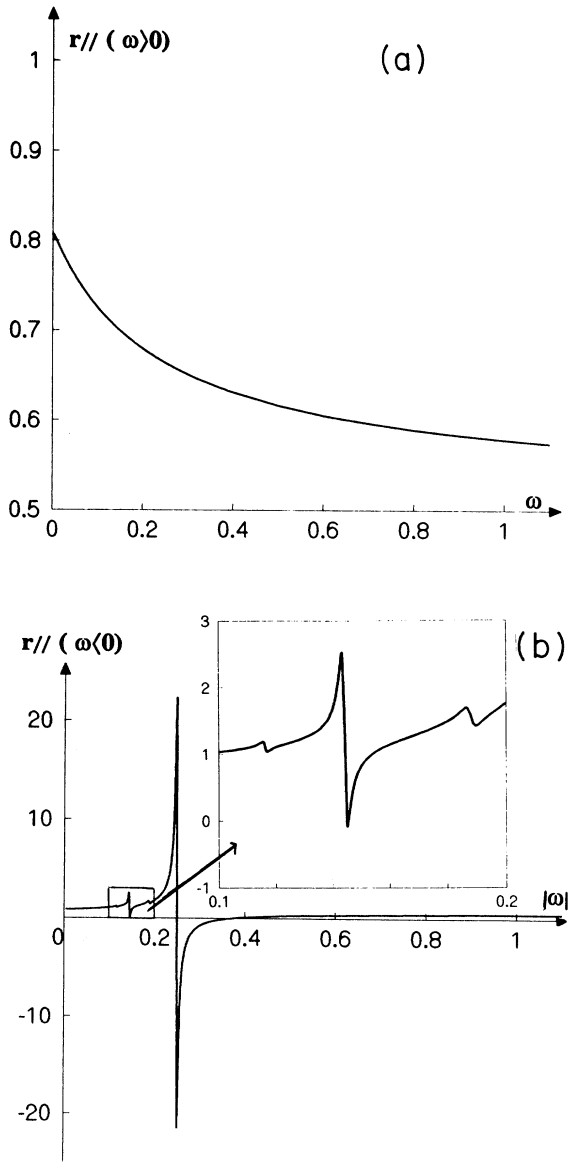

FIG. 7. $r_{\parallel}(\omega)$ versus ω (in units of 10^{14} Hz) for sapphire: (a) $\omega>0$ and (b) $\omega<0$.

TABLE III. Theoretical values for the surface vW coefficient associated to the $6S_{1/2}$-$7P_{3/2}$ Cs transition, for different limiting cases of the birefringent sapphire, compared to the experimental estimate.

	C_3 (kHz μm^3)
Calculated	
$C_3^{\parallel}$ (approximate)	13.81
(exact)	13.81
Calculated	
$C_3^{\perp}$ (approximate)	13.81
(exact)	13.80
Calculated	
$\bar{C}_3$ (birefringent)	13.81
Measured	
[18]	20 (4)

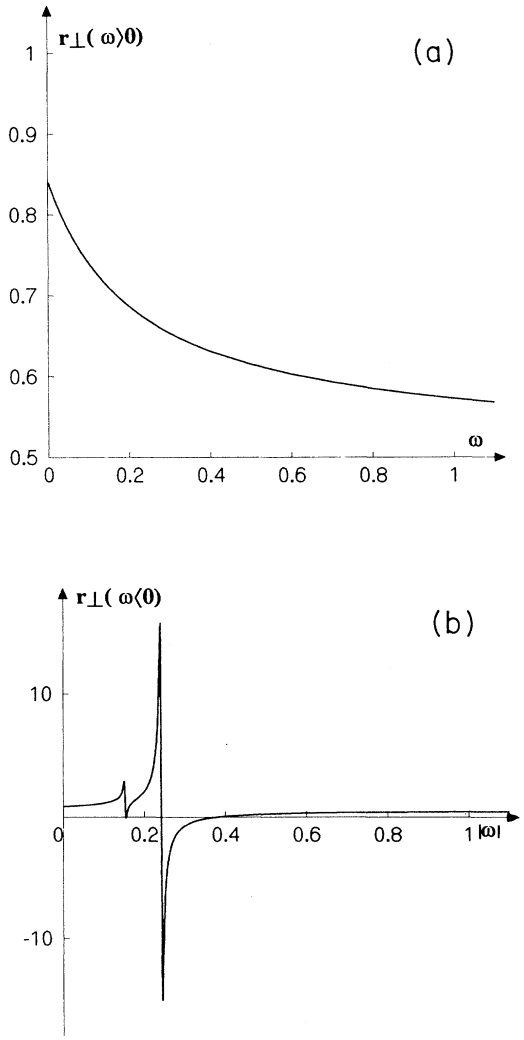

FIG. 8. $r_{\perp}(\omega)$ versus ω (in units of 10^{14} Hz) for sapphire: (a) $\omega > 0$ and (b) $\omega < 0$.

vW attraction, quite independent of the window birefringence and of the various approximate models (see Table III). The calculated value is on the order of 14 kHz μm^3, in better agreement with the experimental determination (20 kHz μm$^3 \pm 25\%$) than the previous crude theoretical estimation (11 kHz μm^3) [18]. One notes that, as all major couplings are the virtual absorption type, it excludes the possibility of a resonantly magnified vW interaction. This also explains why the birefringent nature of sapphire does not sensitively affect the theoretical predictions.

Conversely, for the $6D$ level of Cs, which is, as already mentioned, strongly coupled to the $7P$ level, the coupling

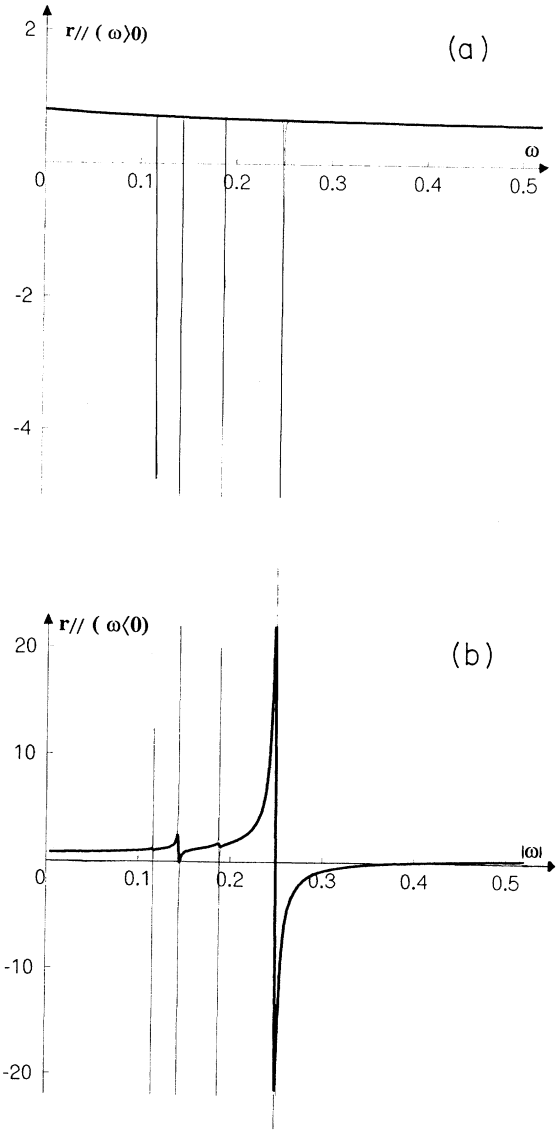

FIG. 9. $r_{\parallel}(\omega)$ versus ω (in units of 10^{14} Hz) for sapphire: (a) $\omega > 0$ and (b) $\omega < 0$. Thick line, exact values (numerical integration); thin line, approximate closed-form expressions. Note that outside the resonances, the closed-form predictions exactly coincide with the numerical calculations.

is now turned into an emission coupling. Table IV lists the main atomic couplings to the $6D$ level with their respective vW contribution in the case of a perfect reflector and in the case of a sapphire window. One notices that the $6D_{3/2} \rightarrow 7P_{1/2}$ coupling ($\lambda = 12.15$ μm), which accounts only for 20% of the overall vW attraction in front of an ideal metal, becomes totally dominant in the case of a sapphire surface and should lead to a magnified surface interaction *whose sign depends on the model.* The theoretical approach, fully taking into account the birefringent behavior of the sapphire window (Sec. II D), predicts a resonantly enhanced vW *repulsion* for the $6D_{3/2}$ level (last column of Table IV).

It is also remarkable that the $6D_{5/2}$ level, very similar to the $6D_{3/2}$ level as far as the atomic structure and energy are concerned, does not feature such a dramatic model-dependent behavior in the sapphire case, although the *bulk* sapphire absorption is much more important than for the $6D_{3/2}$-$7P$ transition. This illustrates how the dielectric medium resonances are affected by the *surface form factor* $(\varepsilon-1)/(\varepsilon+1)$.

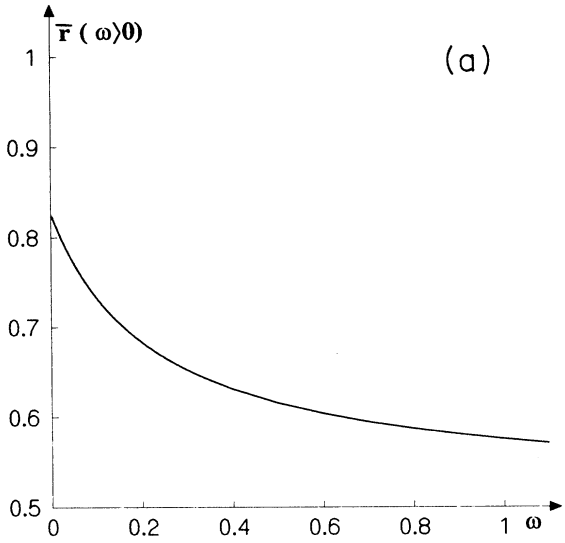

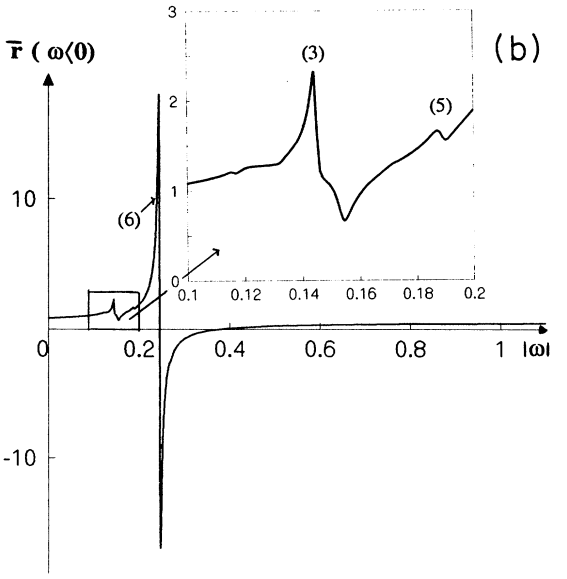

FIG. 10. $\bar{r}(\omega)$ versus ω (in units of 10^{14} Hz) for the birefringent sapphire: (a) $\omega > 0$ and (b) $\omega < 0$.

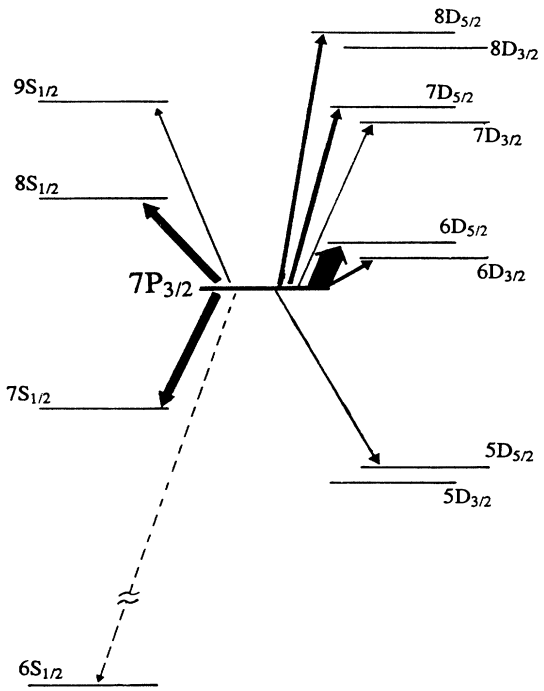

FIG. 11. Schematic representation of the Cs energy diagram, showing the various virtual dipole couplings of the $7P_{3/2}$ level. The thickness of the arrows is approximately proportional to the strength of the coupling contribution to the vW shift for the perfect reflector.

VI. CONCLUSION

In this article, we have analyzed the nonretarded vW interactions between an atom in an arbitrary energy level and a dispersive dielectric surface. We have derived integral and closed-form expressions directly applicable to recent selective reflection experiments. As an example, this approach has been used to analyze the long-range interactions between excited cesium and sapphire.

A major prediction of this study is that atom-surface interactions may be resonantly enhanced when some of the atom emission frequencies are resonant with the dielectric absorption bands. This can lead to giant attraction or repulsion of the excited atom by the dispersive dielectric surface. One should note, however, that, simultaneously to this enhancement of the surface-induced level shift, an enhanced line broadening is also predicted, diverging like $1/z^3$ at short distances and proportional to

TABLE IV. List of the main contributions to the surface vW interaction for the $6D$ Cs levels (in kHz μm^3). The ideal reflector and various limiting cases for birefringent sapphire are considered. Atomic data are taken from [26]. The sign (−) in column 2 is for *emission* coupling.

Levels $a \Longrightarrow a'$		$\lambda_{aa'}$ (μm)	Perfect reflector	Ordinary sapphire	Extraordinary sapphire	Birefringent sapphire
$6D_{5/2} \Longrightarrow$	$6P_{3/2}$	(−)0.918	0.44	0.22	0.22	0.22
	$7P_{3/2}$	(−)14.59	8.05	16	19	17
	$8P_{3/2}$	3.17	0.47	0.27	0.27	0.27
	$4F$	5.44	12.43	7.6	7.6	7.6
	$5F$	2.30	0.33	0.19	0.19	0.19
	$6F$	1.76	0.18	0.10	0.10	0.10
C_3 ($6D_{5/2}$)			22	24	27	25
$6D_{3/2} \Longrightarrow$	$6P_{1/2}$	(−)0.876	0.32	0.16	0.16	0.16
	$7P_{1/2}$	(−)12.15	3.87	75	−44	−61
	$7P_{3/2}$	(−)15.58	1.63	2.5	2.9	2.6
	$8P_{1/2}$	3.21	0.41	0.24	0.23	0.24
	$4F_{5/2}$	5.31	11.60	7	7	7
	$5F_{5/2}$	2.28	0.33	0.19	0.19	0.19
	$6F_{5/2}$	1.74	0.18	0.1	0.1	0.1
C_3 ($6D_{3/2}$)			19	85	−33	−50

$f(\omega)=\mathrm{Im}[(\varepsilon-1)/(\varepsilon+1)]$ [12,27]. Indeed, because of the imaginary part of the dielectric constant, the image dipole has a component out of phase with the atomic dipole, introducing a dissipation process in the dipole-dipole interaction. This near-field divergence of the line broadening, which does not exist for perfect conductors or transparent dielectrics, may reduce the excited-state lifetime notably and partly hinder the observation of such level shift enhancements.

The above situation represents a case study of a strong interaction between an excited microscopic system and a macroscopic ("classical") dielectric body, or, in other words, an example of resonant coupling between a discrete quantum level (initial excited-state atom and ground-state dielectric) and an energy continuum (deexcited atom and excited dielectric). Selective-reflection spectroscopy [16–18] offers a unique means of exploring this type of resonant interaction, by using an excited atomic system as a selective detector of the quantum response of the dielectric-vacuum interface at a set of discrete atomic frequencies.

It should be quite interesting to check the influence of birefringence in the dielectric response. As noted for the case of sapphire, birefringence introduces distinct features for atomic frequencies inside the dielectric absorption bands. In this respect, the $6D_{3/2}$ Cs level should represent a stringent test of the birefringent behavior.

An interesting extension of this work lies in the analysis of the retarded, long-range, interaction between excited atoms and dispersive dielectrics, with such questions like the possible existence of an oscillatory behavior of the atom-surface potential or its interferometric cancellation at a given separation. Other extensions include the excited-atom–dielectric-microsphere interactions around the absorption bands.

APPENDIX A: THE BINARY INTERACTION LIMIT

It is illuminating from a theoretical point of view to derive the well-known binary vW potential [28] between two atoms of different species from our general expression (13). To do so, we assume that the atoms of the dielectric do not interact with each other and we only consider binary interactions of these atoms with the atom outside the dielectric. This amounts to making, for the dielectric, the low-density approximation

$$\frac{\varepsilon-1}{\varepsilon+1}\rightarrow\frac{1}{2}(\varepsilon-1)=2\pi N\alpha_D \ , \tag{A1}$$

where N is the number density of atoms in the dielectric and α_D is the polarizability of one of its atoms. For the polarizability of an arbitrary atom inside the dielectric we introduce the expression

$$\alpha_D(\omega)=\frac{e^2}{m}\sum_{d'}\frac{f_{dd'}}{\omega_{dd'}^2-\omega^2-i\gamma_{dd'}\omega} \ , \tag{A2}$$

where d labels the ground state of the atom and d' designates any state connected to the ground state by a virtual transition with frequency $\omega_{dd'}$ and damping constant $\gamma_{dd'}$.

With our approximation [Eq. (A1)], we then have

$$f(\omega)=\mathrm{Im}\frac{\varepsilon-1}{\varepsilon+1}=\frac{2\pi Ne^2}{m}\frac{f_{dd'}\gamma_{dd'}\omega}{(\omega_{dd'}^2-\omega^2)^2+\gamma_{dd'}^2\omega^2}$$

if we restrict ourselves to one single transition $|d\rangle\rightarrow|d'\rangle$. This expression can be identified with Eq. (22) if we set

$$K_1=2\pi N\frac{e^2}{m}f_{dd'}\gamma_{dd'} \ , \quad \gamma_1=\gamma_{dd'} \ , \quad \Omega_1=\omega_{dd'} \ .$$

Then, with the result of Eq. (26), we find the expression

$$\mathrm{P}\int_0^\infty \mathrm{Im}\frac{\varepsilon(\omega)-1}{\varepsilon(\omega)+1}\frac{1}{\omega_0^2-\omega^2}d\omega=\pi^2 N\frac{e^2}{m}\frac{f_{dd'}}{\omega_{dd'}}\frac{1}{\omega_0^2-\omega_{dd'}^2} .$$

With the same type of approximations, i.e., $\gamma_{dd'}$ small compared with all characteristic frequencies, we have, using Eqs. (A1) and (A2),

$$\mathrm{Re}\frac{\varepsilon(\omega_0)-1}{\varepsilon(\omega_0)+1}=2\pi N\frac{e^2}{m}f_{dd'}\frac{1}{\omega_{dd'}^2-\omega_0^2} .$$

Hence Eq. (11) yields the expression

$$r(\omega_0)=2\pi N\frac{e^2}{m}f_{dd'}\frac{\omega_0}{\omega_0^2-\omega_{dd'}^2}\left[\frac{1}{\omega_{dd'}}-\frac{1}{\omega_0}\right]$$
$$=2\pi N\frac{e^2}{m}f_{dd'}\frac{1}{\omega_{dd'}(\omega_0+\omega_{dd'})} .$$

By substituting this result into Eq. (13), with $\omega_0=\omega_{en'}$, we find

$$V(z)=-\frac{\pi}{6}\frac{e^2}{m}N\frac{1}{z^3}\sum_{n',d'}|\mu_{en'}|^2 f_{dd'}\frac{1}{\omega_{dd'}(\omega_{en'}+\omega_{dd'})} .$$

By introducing the oscillator strength $f_{en'}$ defined by the relation

$$f_{en'}=\frac{2}{3}\frac{m}{\hbar e^2}\omega_{en'}|\mu_{en'}|^2 ,$$

we write $V(z)$ in the form

$$V(z)=-\frac{\pi}{4}\hbar\frac{e^4}{m^2}N\frac{1}{z^3}\sum_{n',d'}\frac{f_{en'}f_{dd'}}{\omega_{en'}\omega_{dd'}(\omega_{en'}+\omega_{dd'})} . \quad \text{(A3)}$$

This result can easily be related to the binary vW potential between two atoms at distance R, as given by the expression

$$V_6(R)=-\frac{C_6}{R^6} .$$

Then, by summation over binary interactions between the atom outside and all the atoms inside the dielectric one obtains, for the constant C_6, the relation $C_6=(6/\pi)(1/N)C_3$, with C_3 defined by the relation $V(z)=-C_3/z^3$. By extracting C_3 from Eq. (A3) we thus find

$$C_6=\frac{3}{2}\hbar\frac{e^4}{m^2}\sum_{n',d'}\frac{f_{en'}f_{dd'}}{\omega_{en'}\omega_{dd'}(\omega_{en'}+\omega_{dd'})}$$
$$=\frac{3}{2}\frac{e^4}{m^2}\frac{h}{(2\pi)^4}\sum_{n',d'}\frac{f_{en'}f_{dd'}}{\nu_{en'}\nu_{dd'}(\nu_{en'}+\nu_{dd'})} .$$

This well-known result [29] has been widely used for calculating vW constants for ground- and excited-state potentials.

APPENDIX B: APPROXIMATE CALCULATION IN THE CASE OF MULTIPLE RESONANCES

We present a method that allows us to write the quantity $f(\omega)=\mathrm{Im}[(\varepsilon-1)/(\varepsilon+1)]$ as a sum of Lorentzian-type shapes involving N resonances at frequencies Ω_n and linewidth parameters Γ_n, assuming that $\varepsilon(\omega)$ is represented by an expression of the type of Eq. (19). Our method is valid in the case $\gamma_n \ll \omega_n$, i.e., for *narrow lines* in the spectrum of the dielectric. Starting from Eq. (19) we can write

$$F=(\varepsilon-1)/(\varepsilon+1)=\left[C\prod_n(\omega_n^2-\omega^2-i\gamma_n\omega)+\sum_n f_n\omega_n^2\prod_{i\neq n}(\omega_i^2-\omega^2-i\gamma_i\omega)\right]$$
$$\times\left[(C+2)\prod_n(\omega_n^2-\omega^2-i\gamma_n\omega)+\sum_n f_n\omega_n^2\prod_{i\neq n}(\omega_i^2-\omega^2-i\gamma_i\omega)\right]^{-1} . \quad \text{(B1)}$$

According to the approximation stated above we restrict ourselves in both the numerator and the denominator to terms linear in the γ_n. This yields

$$F=\left[C\prod_n(\omega_n^2-\omega^2)+\sum_n f_n\omega_n^2\prod_{i\neq n}(\omega_i^2-\omega^2)-iC\omega\sum_n\gamma_n\prod_{i\neq n}(\omega_i^2-\omega^2)-i\omega\sum_n\sum_{i\neq n}f_n\omega_n^2\gamma_i\prod_{j\neq i,j=n}(\omega_j^2-\omega^2)\right]$$
$$\times\left[(C+2)\prod_n(\omega_n^2-\omega^2)+\sum_n f_n\omega_n^2\prod_{i\neq n}(\omega_i^2-\omega^2)-i(C+2)\omega\sum_n\gamma_n\prod_{i\neq n}(\omega_i^2-\omega^2)-i\omega\sum_n\sum_{i\neq n}f_n\omega_n^2\gamma_i\prod_{j\neq i,j\neq n}(\omega_j^2-\omega^2)\right]^{-1} . \quad \text{(B2)}$$

If we write this expression in the form $F=(A-i\omega B)/(D-i\omega E)$, its imaginary part is given by

$$f(\omega)=\frac{\omega(AE-BD)}{(D^2+\omega^2E^2)} .$$

Now we introduce the roots of the quantity $\varepsilon(\omega)+1$ for the case $\gamma_n=0$ and designate them as Ω_n. Then we obtain, after some algebra, the expression

$$f(\omega)=2\omega\left[\sum_n\gamma_n\prod_{i\neq n}(\omega_i^2-\omega^2)\sum_n f_n\omega_n^2\prod_{i\neq n}(\omega_i^2-\omega^2)-\left[\sum_n\sum_{i\neq n}f_n\omega_n^2\gamma_i\prod_{j\neq i,j\neq n}(\omega_j^2-\omega^2)\right]\prod_n(\omega_n^2-\omega^2)\right]\Big/\mathcal{D} ,$$

where the denominator

$$\mathcal{D}=(C+2)^2\prod_n(\Omega_n^2-\omega^2)^2+\omega^2\left[(C+2)\sum_n\gamma_n\prod_{i\neq n}(\omega_i^2-\omega^2)+\sum_n\sum_{i\neq n}f_n\omega_n^2\gamma_i\prod_{j\neq i,j\neq n}(\omega_j^2-\omega^2)^2\right]^{-1} . \quad \text{(B3)}$$

Finally, the numerator of the right-hand side of this expression can be further reduced so that we have

$$f(\omega)=2\omega\left[\sum_n \gamma_n f_n \omega_n^2 \prod_{i\neq n}(\omega_i^2-\omega^2)^2\right]\Big/\mathcal{D}\ . \tag{B4}$$

With the assumption of small γ_n's, the damping term in the denominator of Eq. (B4) can be considered to be small compared to the distance between resonances as defined by the different values of Ω_n. Under this condition we can write $f(\omega)$ as the sum of N terms, each one describing a resonance centered at frequency Ω_n. The shape of each term can be deduced easily from the structure of Eq. (B4). Hence we can write

$$f(\omega)=\sum_n \frac{K_n\omega}{(\Omega_n^2-\omega^2)^2+\Gamma_n^2\omega^2}\ ,$$

where the parameters K_n and Γ_n are given by the expressions

$$K_n=\frac{2\sum_i \gamma_i f_i \omega_i^2 \prod_{j\neq i}(\omega_j^2-\Omega_n^2)^2}{(C+2)^2\prod_{i\neq n}(\Omega_i^2-\Omega_n^2)^2}\ , \tag{B5}$$

$$\Gamma_n=\frac{\left[(C+2)\sum_i \gamma_i \prod_{j\neq i}(\omega_j^2-\Omega_n^2)+\sum_i f_i\omega_i^2\sum_{j\neq i}\gamma_j \prod_{k\neq i,k\neq j}(\omega_k^2-\Omega_n^2)\right]}{(C+2)\prod_{i\neq n}(\Omega_i^2-\Omega_n^2)}\ . \tag{B6}$$

[1] J. E. Lennard-Jones, Trans. Faraday Soc. **28**, 334 (1932).
[2] J. Bardeen, Phys. Rev. **58**, 727 (1940).
[3] H. B. G. Casimir and D. Polder, Phys. Rev. **73**, 360 (1948).
[4] E. M. Lifshitz, Zh. Eksp. Teor. Fiz. **29**, 94 (1955) [Sov. Phys. JETP **2**, 73 (1956)]; I. E. Dzyaloshinskii, E. M. Lifshitz, and L. P. Pitaevskii, Adv. Phys. **10**, 165 (1961).
[5] C. Mavroyannis, Mol. Phys. **6**, 593 (1963).
[6] A. D. McLachlan, Proc. R. Soc. London Ser. A **271**, 387 (1963); Mol. Phys. **6**, 423 (1963); **7**, 381 (1964).
[7] G. Barton, J. Phys. B **7**, 2134 (1974).
[8] G. S. Agarwal, Phys. Rev. A **11**, 230 (1975); **12**, 1475 (1975).
[9] R. R. Chance, A. Prock, and R. Silbey, Phys. Rev. A **12**, 1448 (1975).
[10] M. Babiker and G. Barton, J. Phys. A **9**, 129 (1976).
[11] E. Zaremba and W. Kohn, Phys. Rev. B **13**, 2270 (1976).
[12] J. M. Wylie and J. E. Sipe, Phys. Rev. A **30**, 1185 (1984); J. M. Wylie and J. E. Sipe, Phys. Rev. **32**, 2030 (1985).
[13] D. Meschede, W. Jhe, and E. A. Hinds, Phys. Rev. A **41**, 1587 (1990); E. A. Hinds and V. Sandoghdar, *ibid.* **43**, 398 (1991).
[14] A. Anderson, S. Haroche, E. A. Hinds, W. Jhe, and D. Meschede, Phys. Rev. A **37**, 3594 (1988).
[15] See, e.g., G. Vidali, G. Ihm, H. Y. Kim, and M. W. Cole, Surf. Sci. Rep. **12**, 133 (1991).
[16] M. Oria, M. Chevrollier, D. Bloch, M. Fichet, and M. Ducloy, Europhys. Lett. **14**, 527 (1991); M. Chevrollier, D. Bloch, G. Rahmat, and M. Ducloy, Opt. Lett. **16**, 1879 (1991); N. Papageorgiou, M. Fichet, V. Sautenkov, D. Bloch, and M. Ducloy, Laser Phys. **4**, 392 (1994).
[17] M. Ducloy and M. Fichet, J. Phys. (France) II **1**, 1429 (1991).
[18] M. Chevrollier, M. Fichet, M. Oria, G. Rahmat, D. Bloch, and M. Ducloy, J. Phys. (France) II **2**, 631 (1992).
[19] See, e.g., J. D. Jackson, *Classical Electrodynamics,* 2nd ed. (Wiley, New York, 1975), pp. 147–149.
[20] See, e.g., L. D. Landau and E. M. Lifshitz, *Physique Statistique* (Editions Mir, Moscow, 1967), pp. 466–473.
[21] T. Kiraha and N. Honda, J. Phys. Soc. Jpn. **20**, 15 (1965).
[22] L. W. Bruch and H. Watanabe, Surf. Sci. **65**, 619 (1977).
[23] To get the field inside an infinite birefringent dielectrics, see, e.g., L. D. Landau and E. M. Lifshitz, *Electrodynamique des Milieux Continus* (Editions Mir, Moscow, 1969), pp. 83–89.
[24] A. S. Barker, Phys. Rev. **132**, 1474 (1963); I. H. Malitson, J. Opt. Soc. Am. **52**, 1377 (1962).
[25] Similar resonant enhancements have been previously predicted for excited atoms [12] or classical dipoles [9] oscillating above a metal surface, described by the Drude model, when the oscillation frequency is close to the plasmon frequency.
[26] A. Lindgard and S. E. Nielsen, in *Atomic Data and Nuclear Tables* (Academic, New York, 1977), pp. 533–633.
[27] R. R. Chance, A. Prock, and R. Silbey, J. Chem. Phys. **62**, 2245 (1975).
[28] J. O. Hirschfelder, C. F. Curtiss, and R. B. Bird, *Molecular Theory of Gases and Liquids* (Wiley, New York, 1974).
[29] E. Lindholm, Ph.D. thesis, Uppsala, 1942.